Journal of Biomolecular NMR (2006) 34: 203–208
DOI 10.1007/s10858-006-0019-5

NMR structure note

Solution structure of the first Src homology 3 domain of human Nck2

Sunghyouk Park[a,b,*], Koh Takeuchi[a] & Gerhard Wagner[a,*]
[a]*Department of Biological Chemistry and Molecular Pharmacology, 240 Longwood Avenue, Boston, MA 02115, USA;* [b]*Department of Biochemistry, College of Medicine, Inha University, Shinheung-dong, Chung-gu Incheon, Korea 400-712,*

Received 15 November 2005; Accepted 23 January 2006

Key words: CD3ε, Nck, NMR, SH3 domain

Biological context

Nck is an adaptor protein with three N-terminal SH3 domains and one C-terminal SH2 domain. Nck is known for its role in the actin cytoskeleton modulation in T-cell activation. Upon T-cell receptor (TCR) engagement, the adaptor Nck binds the cytoplasmic tail of CD3ε, a component of the invariant part of the TCR complex, and recruits several other proteins, engaging a complex network of protein interactions (Lin and Weiss, 2001). The signaling event involves Nck's interaction with SLP-76, another adaptor molecule that is phosphorylated by ZAP-70 protein kinase. SLP-76 also binds Vav, and the Nck–SLP76–Vav complex activates WASP. The activated WASP starts the cytoskeletal modulation by enhancing the actin nucleation activity of ARP2/3. The exact sequence of the signaling events involving the Nck, however, is still a point of much debate as judged from several recent contradicting reports (Gil et al., 2002; Barda-Saad et al., 2005; Szymczak et al., 2005).

There are two isoforms, Nck1 and Nck2, with high sequence homology (44% identity and 65% similarity) and an equivalent line up of domains. In addition, the SH3 domains within either Nck1 or Nck2 have high sequence similarity. Despite the similarities, there are differential biological activities for the two proteins and their domains recognize different ligands. For example, even with 85% sequence identity, Nck2-SH2 binds ephrin-B but Nck1-SH2 does not (Cowan and Henkemeyer, 2001). In addition, out of the three SH3 domains, only the first SH3 domain binds CD3ε. These specificities of individual domains were reviewed recently (Buday et al., 2002). However, the structural or mechanistic bases of these differences are not well understood.

As a first step to understand the specificities of the Nck domains, we solved the structure of the first SH3 domain of Nck2 and identified residues involved in the interaction with CD3ε.

Methods and results

The human Nck (Nck2) gene was purchased from Open Biosystems (Huntsville, AL). The CD3ε peptide corresponding to the proline rich sequence of the cytoplasmic tail was synthesized at the Biopolymer laboratory of Harvard Medical School. The peptide has the sequence of QRGQNKERPPPVPNPDY. The gene for the first SH3 domain was amplified using the following primers containing *Nde*I and *Xho*I restriction sites:

*To whom correspondence should be addressed. E-mail: spark@inha.ac.kr or gerhard_wagner@hms.harvard.edu

GATGACAAGCATATGACAGAAGAAGTTATTGTGATAGCC (sense),
CGAAACTCCTCGAGCTTCCGCTCCACGTAGTTGGAC (antisense).

The PCR product was cloned into the corresponding restriction sites in the pET30b vector from Novagen (Madison, WI) and transformed into Rosetta(DE3)pLysS *Escherichia coli* strain. All the clones were verified by DNA sequencing.

The protein was isotopically labeled (^{15}N, ^{13}C or in combination) by growing the *E. coli* in M9 minimal medium (typically, 2 l) with ^{15}N NH_4Cl (1 g/l) and ^{13}C-glucose (2 g/l) as sole nitrogen and carbon sources depending on the labeling requirement. The culture was grown at 37 °C to log phase and 1 mM IPTG was added to induce the protein. After 4 h of induction, the culture was harvested by centrifugation. The cell pellets were resuspended in lysis buffer (50 mM sodium phosphate, 300 mM NaCl,10 mM imidazole, pH 8.0) with Complete EDTA-Free protease inhibitor (Roche, Indianapolis, IN). The cells were lyzed by sonication applying four 1-min runs of pulsing separated by 30 s interval. The cell lysate was spun down to remove the insoluble cellular debris. The cleared supernatant was mixed with 7 ml of Ni-NTA (50% slurry) and washed with 200 ml washing buffer (50 mM sodium phosphate, 300 mM NaCl, 20 mM imidazole, pH 8.0). The protein was eluted from the resin with 40 ml of elution buffer (50 mM sodium phosphate, 300 mM NaCl, 250 mM imidazole, pH 8.0). Subsequently, the protein was concentrated with an Amicon ultra device (5 kDa MWCO, Millipore, Billerica, MA). All the NMR experiments were carried out at 25 °C and the samples were prepared in 50 mM sodium phosphate buffer (pH 6.5) and 50 mM EDTA. Protein concentrations were determined from absorbance at 280 nm, by using extinction coefficients calculated from the primary sequence.

The initial protein sample turned out to be a mixture of dimers and monomers without any significant presence of higher oligomers, as judged by gel filtration. The ^{1}H–^{15}N HSQC spectrum of the sample also displayed many more peaks than expected from the sequence, suggesting the presence of at least two states in slow exchange, such as monomer and dimer. Therefore, the putative monomer was separated by gel filtration on a Superdex-75 column (Amersham biosciences, Piscataway, NJ) and then concentrated again. The purified and re-concentrated monomer sample did not have appreciable contamination from the dimer and showed much fewer peaks than the mixture, which is consistent with a monomer. The concentrated ($\sim$600 μM) monomeric sample was stable for about 3 months, after which the dimer peaks started to appear in the ^{1}H–^{15}N HSQC. Considering this very slow time scale of exchange and the absence of cysteine residues in the protein, we suspect that a domain-swapped dimer forms with time, similar to that found previously in another SH3 domain (Kishan et al. 2001). However, this would require additional experimental evidence to confirm.

NMR data were acquired using Bruker DRX 500, Varian Inova 500 and Varian Inova 600 machines equipped with gradient triple resonance and cryogenic probes.

Sequential assignments of the backbone resonances were obtained using HNCACB and CBCA(CO)NH, and sidechain assignments were obtained using H(CCO)NH, C(CO)NH, HCCH-TOCSY spectra (for a review see Ferentz and Wagner, 2000). Stereospecific assignments for the diastereotopic methyl groups were obtained using constant time HSQC on a 10% ^{13}C labeled sample (Neri et al., 1989). All the raw data were processed using nmrPipe (Delaglio et al., 1995) and the processed data were analyzed using the nmrview (Johnson and Blevins, 1994) software.

All the backbone amide resonances were assigned (Figure 1) except for N54, which does not show a peak in the HSQC. Most of the non-labile proton sidechain resonances were also assigned. The assignments were deposited in the BMRB database (accession number 6854). The 3-D protein structure was calculated based on various experimentally derived NOE constraints and TALOS angle restraints (Cornilescu et al., 1999) (Table 1). Peak intensities were categorized as strong, medium, weak and very weak with upper distance bounds set to 3.4, 4.0, 5.5, and 6.5 Å, respectively. For non-stereospecifically assigned diastereotopic protons and aromatic and methyl homotopic protons, the ambiguous distance constraints were used. The lower distance bounds were set to 1.8 Å in all distance categories. Initial structures were obtained using the CYANA program (Guntert et al., 1997) and the final structures were calculated using the CNS program (Brunger et al., 1998), implementing the conformational databases and the secondary

chemical shift database described earlier (Kuszewski et al., 1997). For the final structure, the 30 lowest-energy models without any distance (> 0.3 Å) and dihedral angle (> 5°) violations were selected. The structures were deposited to the RCSB database with accession number 2B86.

The calculated structure showed that the Nck-SH3 domain has a canonical SH3 fold (Figure 2). The structure consists of a 5 stranded beta barrel connected by the 3 canonical loops (distal, RT and n-Src loop) found in many other SH3 domains. While the beta stranded regions are quite tightly converged, there are two regions, around residue 15–19 (part of the RT loop) and 52–56, with some minor alternate conformations. These regions showed signs of conformational exchange in ^{13}C-dispersed NOESY spectra with split or weak intensity peaks. Therefore, the larger structural disorder of these regions in the calculated structure seems to be due to genuine conformational heterogeneity. Although there is one proline residue (P52) in these regions, it is solely in the *trans* conformation, as confirmed with a NOESY spectrum, and it does not contribute to the conformational exchange.

The first SH3 domain of Nck can bind CD3ε whereas the second and the third SH3 domain cannot. To confirm the binding and to identify the residues involved in the interaction with CD3ε, a HSQC binding experiment was carried out. The result showed that the Nck-SH3 domain uses similar residues for binding the proline rich ligand as other SH3 domains (Figure 2c and supplementary Figure S2).

Discussion and conclusion

The first SH3 domain of the Nck is a genuine SH3 domain with most of the common features in an SH3 domain. For the primary structure, it has the WW sequence motif at the beginning of the Cβ

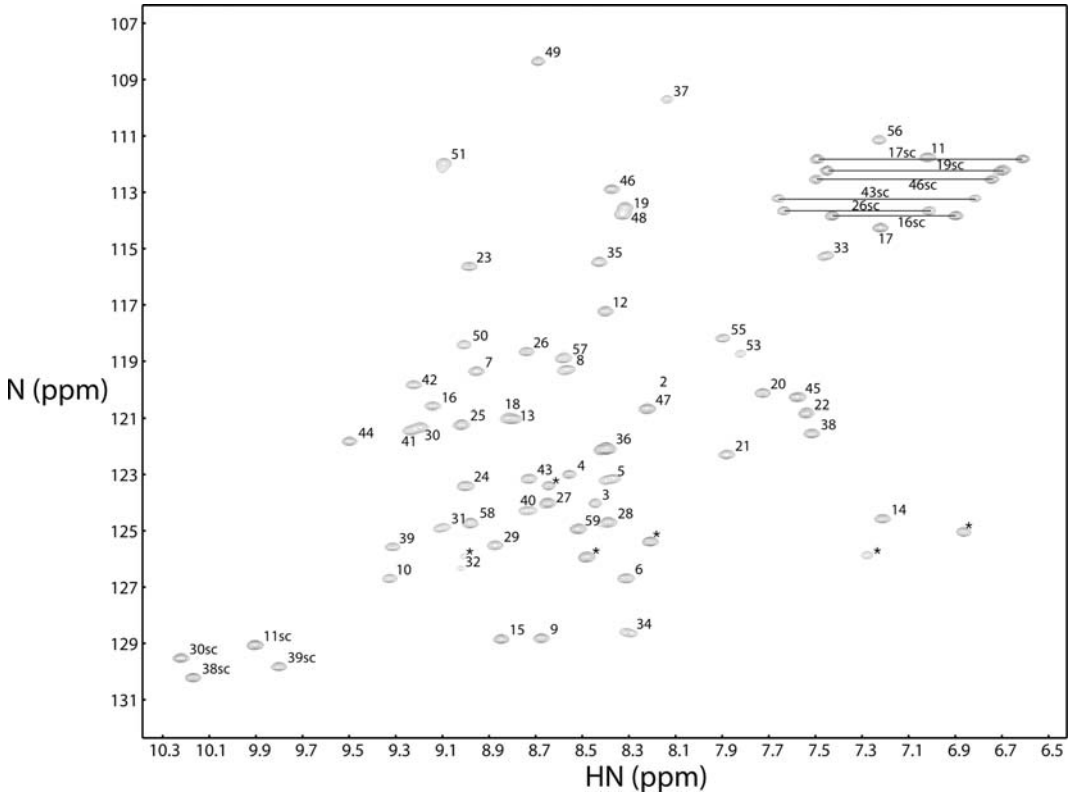

Figure 1. ^{1}H–^{15}N HSQC spectrum of the first Nck-SH3 domain with sequence-specific assignments. The resonances of the sidechain NH_2 or the tryptophan indole groups are labeled with residue number followed by "sc". The peaks with asterisks are those from either aliased arginine sidechains or the C-terminal non-natural residues inserted due to the cloning.

strand and the PXXY motif between the Dβ and the Eβ strands. It also has the sequence similar to the so-called ALYDY motif (AKWDY here). Interestingly, the ALYDY motif is not readily detectable in the second and the third SH3 domains of Nck in the multiple sequence alignment including other SH3 domains (see supplementary Figure S1).

To check the common SH3 domain features in the 3-dimensional structures, the calculated structure was compared with other SH3 domains important in TCR signaling, namely those of Fyn (pdb code: 1FYN) and Lck (pdb code: 1H92) (Figure 3). The structures overlap nicely with each other (the DALI Z-scores are 8.0 for Fyn and 7.4 for Lck SH3) (Holm and Sander, 1993). Nevertheless, the CD3ε peptide does not bind appreciably to Fyn or Lck SH3 domains (data not shown). The capability to bind CD3ε might differentiate Nck from Fyn and Lck, similarly to the mechanisms suggested for the differential binding to a proline rich sequence in CD2 by Fyn and Lck (Freund et al., 2002). It would be interesting to see if the replacement of the RT loop sequence of the Nck first SH3 domain in Fyn or Lck confers binding affinity to the CD3ε peptide.

We have shown that the proline-rich peptide of the CD3ε cytoplasmic tail binds the canonical binding motif (Musacchio, 2002) in the first SH3 domain of Nck. As described above, the Nck has three SH3 domains and each binds different proline-rich ligands with remarkable specificity. The three dimensional structure for the first (reported here) and the third SH3 domain (reported previously, pdb code: 1WX6) are very similar with DALI Z-core of 6.3 (Figure 3c). One possible explanation of this substrate specificity for the first SH3 domain could have been that it uses a non-canonical binding site not found in the other SH3 domains. It is worth noting that the third Nck-SH3 domain uses non-canonical sites for its interaction with the LIM4 domain of PINCH1, and that the LIM4 domain does not have a canonical PXXP motif (Vaynberg et al., 2005). This might suggest, at least in part, the involvement of non-canonical interactions in the specificity mechanism of Nck-SH3 domains. However, our results exclude the use of non-canonical sites in the first Nck-SH3 domain/CD3ε interaction. Thus, it seems that the specificity is due to either a subtle sequence difference in the ligand-binding regions (especially, the RT loop region) or *cis*-acting regulation of the domain–ligand interaction by other parts of the Nck molecule. The former mechanism has been observed in the Abl protein kinase SH3 domain where the SH3 domain uses a threonine residue in the RT loop region instead of the more common Asp or Glu, to convey the specific binding to its cognate binding partner. The latter mechanism is related to the maintenance of the Src protein kinase in the inactive state by the intra-molecular interaction between the SH3 domain and an internal proline-rich sequence. An intra-molecular interaction as the mechanism of ligand binding specificity was also reported recently in the case of a tandem repeat of PDZ domains (Long et al., 2005). Elucidating the exact features of the specificity will be crucial for understanding the mechanisms responsible for switching between different T-cell signaling pathways.

Table 1. Statistics of the calculated structures of the first SH3 domain of Nck

Number of NOE distance constraints	
Total	1017
Intra-residue	436
Short or Medium ($1 \leq \lvert i-j \rvert \leq 4$)	271
Long ($5 \leq \lvert i-j \rvert$)	310
Number of dihedral angle restraints (backbone ϕ and ψ)	60
RMSD from ideal covalent geometry	
Bonds (Å)	0.005107 ± 0.000591
Angles (degrees)	0.46 ± 0.026
Improper torsion angles (degrees)	0.3460 ± 0.0283
Quality check by PROCHECK-NMR[a]	
Most favored regions	90.8%
Additional allowed regions	9.2%
Generously allowed regions	0.0%
Residues in disallowed regions	0.0%
RMSD from mean structure[b] (Å)	
Backbone atoms	0.314
All heavy atoms	0.860

[a]As stated in the Materials and methods section, structures were calculated including the use of conformational databases, which drives structures towards the most favored regions.[b]Residues 4–57.

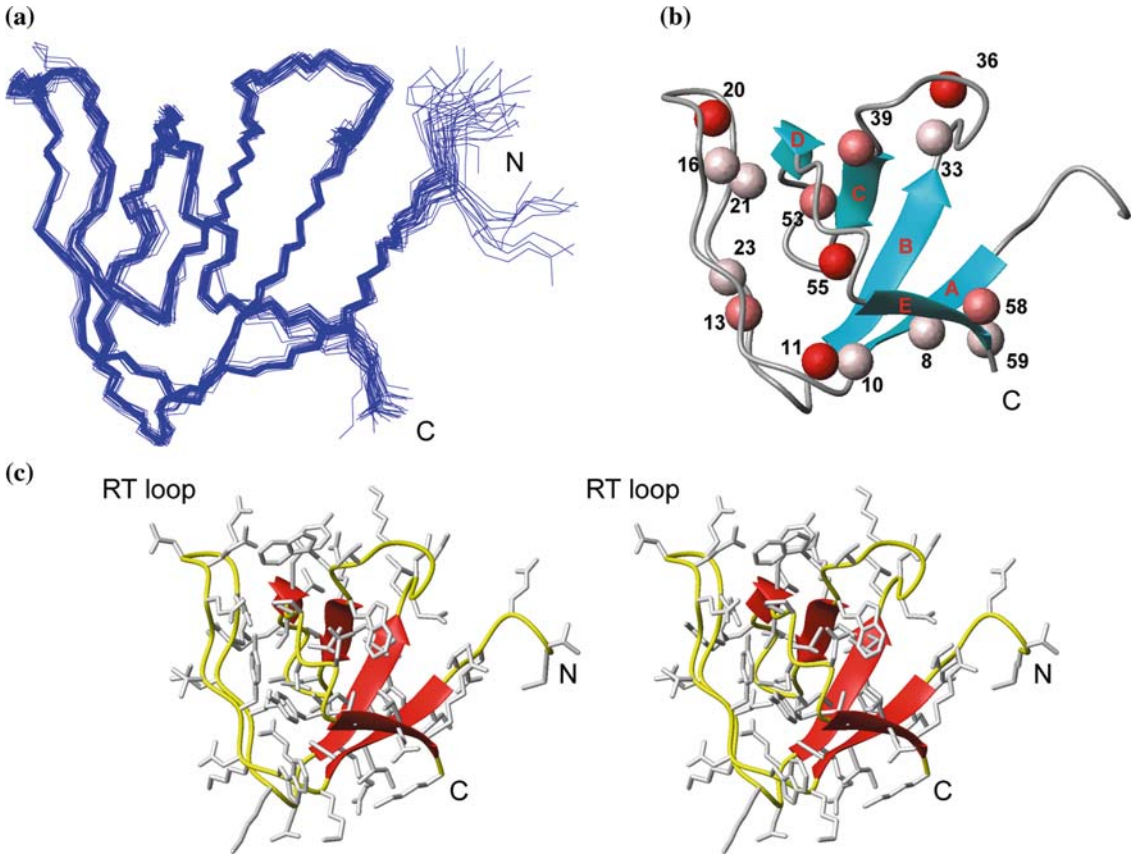

Figure 2. Calculated structure of the first SH3 domain of Nck. (a) Ensemble of the 30 lowest energy conformers without distance (> 0.3 Å) or angle (> 5°) violations. The structural models were aligned for the backbone atoms of residues 4–57. (b) Stereoview of the ribbon diagram of the backbone and a rod representation of side chain heavy atoms for a representative structure. (c) The binding sites for the CD3εγ, as determined by the chemical shift mapping. The balls represent the shifted residues and the color scale is according to the normalized chemical shift changes (see also the supplementary Figure S2): Dark (> 0.2 ppm), Medium (> 0.1 ppm), Light (> 0.08 ppm and < 0.1 ppm).

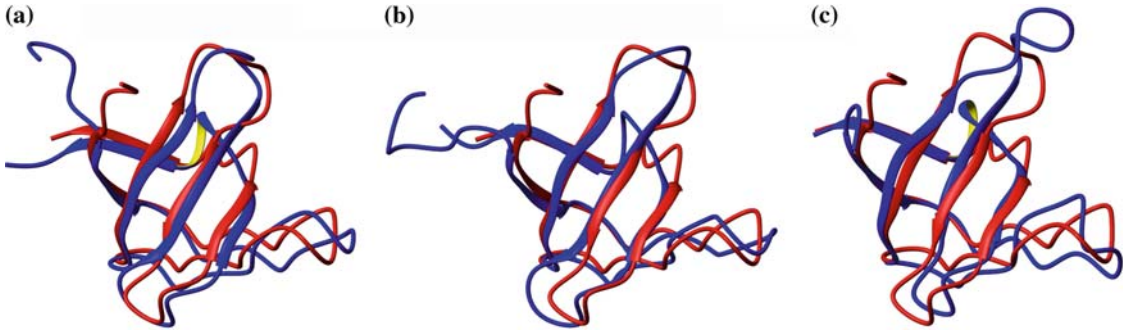

Figure 3. Structure comparison of the first SH3 domain of Nck with those of Fyn (1FYN), Lck (1H92) and the third SH3 domain of Nck (1WX6). The backbone heavy atoms of each molecule were aligned to minimize the RMSD. The backbone atoms for the alignment were selected based on the multiple sequence alignment shown in the supplementary Figure S1. (a) Alignment of Nck and Fyn; residues 2–33, 34–48, 49–59 (for Nck-SH3) and residues 81–112, 114–128, 130–140 (for Fyn-SH3) were used. (b) Alignment of Nck and Lck; residues 7–46, 47–58 (for Nck-SH3) and residues 9–48, 50–61 (for Lck-SH3) were used. (c) Alignment of the first and the third SH3 domains of Nck; residues 3–33, 34–37, 38–43, 45–48, 49–58 (first SH3 domain) and residues 16–46, 48–51, 54–59, 60–63, 65–75 (third SH3 domain, residue numbers are according to 1WX6) were used. The first SH3 domain of Nck is drawn in red and the others are in blue.

Acknowledgements

This work was supported by grants from NIH (GM47467 and AI37581 to GW) and by INHA UNIVERSITY (Research Grant INHA-32729-01 to SP). KT is supported by fellowship from Astellas Foundation for Research on Metabolic Disorders. Maintenance of some of the instruments used for this research was supported by NIH grant EB002026.

Electronic supplementary material is available in electronic format at http://dx.doi.org/10.1007/s10858-006-0019-5

References

Barda-Saad, M., Braiman, A., Titerence, R., Bunnell, S.C., Barr, V.A. and Samelson, L.E. (2005) *Nat. Immunol.*, **6**, 80–89.

Brunger, A.T., Adams, P.D., Clore, G.M., DeLano, W.L., Gros, P., Grosse-Kunstleve, R.W., Jiang, J.S., Kuszewski, J., Nilges, M., Pannu, N.S., Read, R.J., Rice, L.M., Simonson, T. and Warren, G.L. (1998) *Acta. Crystallogr. D. Biol. Crystallogr.*, **54**, 905–921.

Buday, L., Wunderlich, L. and Tamas, P. (2002) *Cell Signal*, **14**, 723–731.

Cornilescu, G., Delaglio, F. and Bax, A. (1999) *J. Biomol. NMR*, **13**, 289–302.

Cowan, C.A. and Henkemeyer, M. (2001) *Nature*, **413**, 174–179.

Delaglio, F., Grzesiek, S., Vuister, G.W., Zhu, G., Pfeifer, J. and Bax, A. (1995) *J. Biomol. NMR*, **6**, 277–293.

Ferentz, A.E. and Wagner, G. (2000) *Quart. Rev. Biophys.*, **33**, 29–65.

Freund, C., Kuhne, R., Yang, H., Park, S., Reinherz, E.L. and Wagner, G. (2002) *EMBO J.*, **21**, 5985–5995.

Gil, D., Schamel, W.W., Montoya, M., Sanchez-Madrid, F. and Alarcon, B. (2002) *Cell*, **109**, 901–912.

Güntert, P., Mumenthaler, C. and Wüthrich, K. (1997) *J. Mol. Biol.*, **273**, 283–298.

Holm, L. and Sander, C. (1993) *J. Mol. Biol.*, **233**, 123–138.

Johnson, B.A. and Blevins, R.A. (1994) *J. Biomol. NMR*, **4**, 603–614.

Kishan, K.V., Newcomer, M.E., Rhodes, T.H. and Guilliot, S.D. (2001) *Protein Sci.*, **10**, 1046–1055.

Kuszewski, J., Gronenborn, A.M. and Clore, G.M. (1997) *J. Magn. Reson.*, **125**, 171–177.

Lin, J. and Weiss, A. (2001) *J. Cell Sci.*, **114**, 243–244.

Long, J.F., Feng, W., Wang, R., Chan, L.N., Ip, F.C., Xia, J., Ip, N.Y. and Zhang, M. (2005) *Nat. Struct. Mol. Biol.*, **12**, 722–728.

Musacchio, A. (2002) *Adv. Protein Chem.*, **61**, 211–268.

Neri, D., Szyperski, T., Otting, G., Senn, H. and Wüthrich, K. (1989) *Biochemistry*, **28**, 7510–7516.

Szymczak, A.L., Workman, C.J., Gil, D., Dilioglou, S., Vignali, K.M., Palmer, E. and Vignali, D.A. (2005) *J. Immunol.*, **175**, 270–275.

Vaynberg, J., Fukuda, T., Chen, K., Vinogradova, O., Velyvis, A., Tu, Y., Ng, L., Wu, C. and Qin, J. (2005) *Mol. Cell*, **17**, 513–523.